Available online at www.sciencedirect.com

SciVerse ScienceDirect

Ceramics International 39 (2013) S373–S377

CERAMICS INTERNATIONAL

www.elsevier.com/locate/ceramint

Fabrication and properties of tricalcium phosphate/barium hexaferrite composites

Narumon Lertcumfu[a], Parkpoom Jarupoom[a,b], Gobwute Rujijanagul[a,*]

[a]Department of Physics and Materials Science, Faculty of Science, Chiang Mai University, Chiang Mai 50200, Thailand
[b]Department of Industrial Engineering, Faculty of Engineering, Rajamangala University of Technology Lanna, Chiang Mai 50300, Thailand

Available online 16 October 2012

Abstract

Beta-tricalcium phosphate based composites containing particles of barium hexaferrite were fabricated. The beta-tricalcium phosphate fine powder was synthesized from egg shell and $Ca_2P_2O_7$ by a solid-state reaction technique. Effects of barium hexaferrite additive (0–3 vol%) on the properties of the composites were investigated. All samples showed a main phase of β-tricalcium phosphate, characterized by X-ray diffraction technique. The additive inhibited grain growth, but enhanced hardness of the composites. M–H hysteresis loops also showed an improvement in the magnetic behavior for higher barium hexaferrite content samples. However, in vitro bioactivity test indicated that the 2 vol% sample may be suitable for biological applications.

Keywords: B. Composite; C. Hardness; D. Ferrite; Solid-state reaction

1. Introduction

Calcium phosphate-based compounds have attracted considerable interest for bioapplications on account of their good properties such as biocompatibility, bioactivity and biodegradability [1]. Hydroxyapatite (HA, $Ca_{10}(PO_4)_6(OH)_2$) is a well known calcium phosphate-based compound where it is the main inorganic component of bone. This material has been widely investigated for many years in the past. HA has been developed for using as bone implants [2]. However, dense HA hinders bone ingrowth after implantation, due to its low biodegradability [3]. Therefore, other materials such as tricalcium phosphate (TCP) are considered for implant applications. Generally, TCP has many phase, such as. α-TCP ($Ca_3(PO_4)_6(OH)_2$)) and β-TCP ($Ca_3(PO_4)_2$) [2]. However, β-TCP is preferred for bioceramic applications due to its mechanical strength, chemical stability, and proper bioresorption rate [1,2]. Generally, the TCP ceramics also exhibit higher resorbable comparing to pure HA. Thus, TCP and HA have been used to form biphasic composites to overcome the low biodegradability of pure HA [4,5].

Unfortunately, poor mechanical properties of β-TCP and the biphasic composite make them unsuitable for load-bearing applications [1]. Therefore, research on improvement of the mechanical properties for the β-TCP ceramics and biphasic composites is still interesting.

Recently, many authors have focused on magnetic materials for biological applications such as MRI contrast agents [6], cell label [7], and hyperthermia for cancer therapy [8].Many magnetic materials have been developed and investigated [8,9]. Barium hexaferrite ($BaFe_{12}O_{19}$, BF) is also one of interesting magnetic materials due to its excellent magnetic properties. BF has a perovskite-like structure with a hexagonal symmetry. This material has a potential for various fields applications [10,11]. Since β-TCP shows good performance for biological applications and BF has excellent magnetic properties, it is interesting to fabricate a composite containing these materials to obtain the optimum properties. To our knowledge, β-TCP/BF composite has not been fabricated and reported before. In the present work, we therefore report the results of our investigation on the properties of the β-TCP/BF composites for the first time.

*Corresponding author. Tel.: +66 53 943376; fax: +66 53 357512.
E-mail address: rujijanagul@yahoo.com (G. Rujijanagul).

0272-8842/$ - see front matter © 2012 Elsevier Ltd and Techna Group S.r.l. All rights reserved.
http://dx.doi.org/10.1016/j.ceramint.2012.10.097

2. Experimental

The starting β-TCP used in this work was prepared via the solid-state method using precursors of calcium pyrophosphate ($Ca_2P_2O_7$, FluKa ≥ 99.0%) and Calcium carbonate (synthesized from egg shell). The egg shell was fird at 625 °C for 3 h. The $Ca_2P_2O_7$ and fired egg shell powders were mixed and ball-milled in the ethanol for 24 h, and then heated at 300 °C for 10 h and 900 °C for 2 h. The obtained powder was calcined in air at 1000 °C for 12 h. In this work, $BaFe_{12}O_{19}$ (BF) was used as the dispersed phase to form the composites. Raw metal oxide of barium oxide ($BaCO_3$, Sigma-Aldrich ≥ 98.5%) and iron oxide (Fe_2O_3, Fluka ≥ 99.0%) was mixed and ball-milled for 24 h. Then, the mixed powder was calcined at 1100 °C for 3 h, with heating and cooling rate of 300 °C/h. The BF powder was formed. The BF powder was mixed with the β-TCP in ratios of between 1.0 and 3.0 vol%. The mixtures were ball milling for 24 h. The obtained powders were uniaxial pressed at 1 MPa into a disc shape. The green body samples were sintered at a temperature of 1250 °C for 2 h. The particle size distribution of β-TCP powder was examined by a dynamic light scattering technique. The phase formation of powder and ceramic samples was carried out by X-ray diffraction technique (XRD). Density of the sintering HA disks was determined by Archimedes method. The microstructure of the samples was examined by a scanning electron microscopy (SEM). Concerning the apatite-forming ability evaluation, the β-TCP/BF composites were immersed in simulated body fluid (SBF) for 14 days (in vitro bioactivity test) [12]. After soaking in SBF, the samples were studied by SEM. For mechanical study, Vickers hardness indentation was performed on surfaces of the composites using a micro hardness tester. Magnetic properties of β-TCP–BF ceramic were measured by a vibrating sample magnetometers (VSM).

3. Results and discussion

XRD pattern of the calcined BF powder is shown in the inset (a) of Fig. 1. The phase formation analysis was carried out based on the JCPDS data file no. 00-039-1433. In the present work, the β-TCP powder was successfully formed when $Ca_2P_2O_7$ and $CaCO_3$ (synthesized from egg shell) were mixed in a ratio of 2:3 and calcined at 1100 °C. XRD pattern of calcined β-TCP is displayed in Fig. 1. Pure phase β-TCP was found where the analysis was carried out based on the JCPDS file No. 00-009-0169. The particle size distribution of β-TCP powder was examined by the dynamic light scattering technique and the result is shown in the in set (b) of Fig. 1. It can be clearly seen that the particle size distribution exhibits a mono-modal distribution. This result suggests no trace of particle agglomeration, implying that the method of powder preparation for the particle size analysis produced a well disperse particles. A narrow particle size between 94 and 289 nm was recorded. The average particle size, as estimated from the particle size analysis was 163 nm. This result suggests that our processing produced a very fine powder of β-TCP.

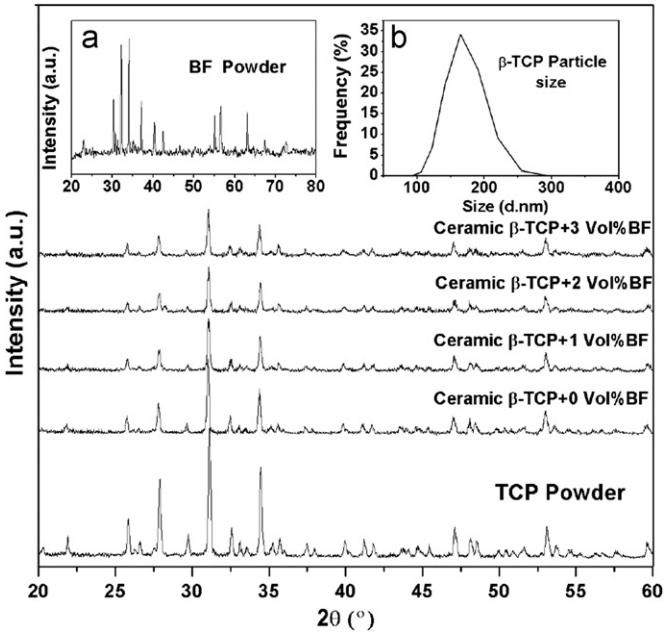

Fig. 1. XRD patterns of undoped and doped TCP samples. Inset (a) shows XRD pattern of BF powder. Inset (b) shows particle size distribution of β-TCP powder.

Fig. 1 also shows the XRD patterns of the composites made from β-TCP and $BaFe_{12}O_9$ mixtures, containing different contents of BF (0.0–3.0 vol%). Although the presence of BF is expected in the higher BF contented samples, the XRD data show that there was only β-TCP phase occurred in the composites. This may be due to the sensitivity limit of this technique. However, intensity of β-TCP peaks decreased with increasing of BF content, suggesting that BF additive had an effect on the degree of crystallinity and/or phase formation of β-TCP in the composites.

The SEM micrographs of the composites were compared with that of pure β-TCP ceramic, as illustrated in Fig. 2. The additive inhibited grain growth, as can be seen from the average grain size in Fig. 3(a), which was reduced from ~5 μm for pure β-TCP to ~3 μm for the 3.0 vol% samples. This reduction may be due to BF particle at the grain boundaries prevented grain boundary movement during the sintering process [13]. For the composites, there was uniformity in grain shape and size across each sample surface, suggesting that the processing method result in uniform distribution of the additive (Fig. 2(c)). Fig. 2(b, d) display SEM micrographs of fracture surfaces for selected samples. The SEM micrographs show a change from an inter-granular fracture in the pure β-TCP ceramic to a partial intragranular (transgranular) cleavage for the composites. The intragranular mode of fracture can be associated with a strengthening of the grain boundaries, which encourages the crack to pass through the grain rather than along the grain boundary. The change in fracture mode may be link to the change in porosity of the composites

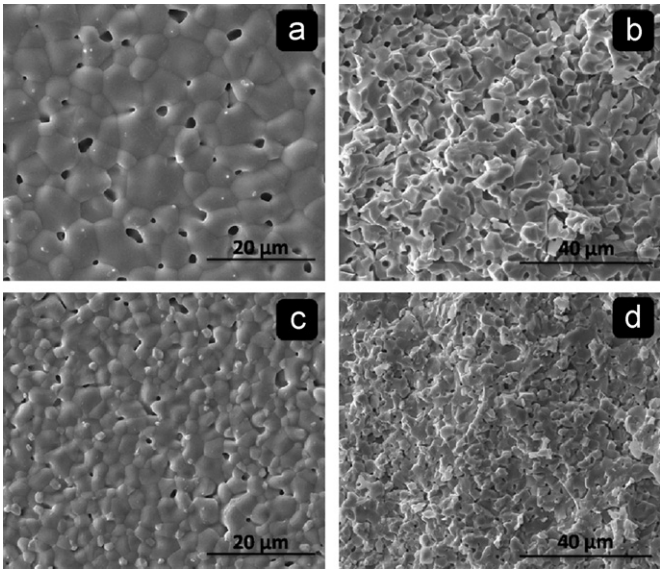

Fig. 2. SEM micrographs of as-sintered and fracture surfaces of samples (a and b) β-TCP ceramic, (c and d) β-TCP −3.0 vol% BF.

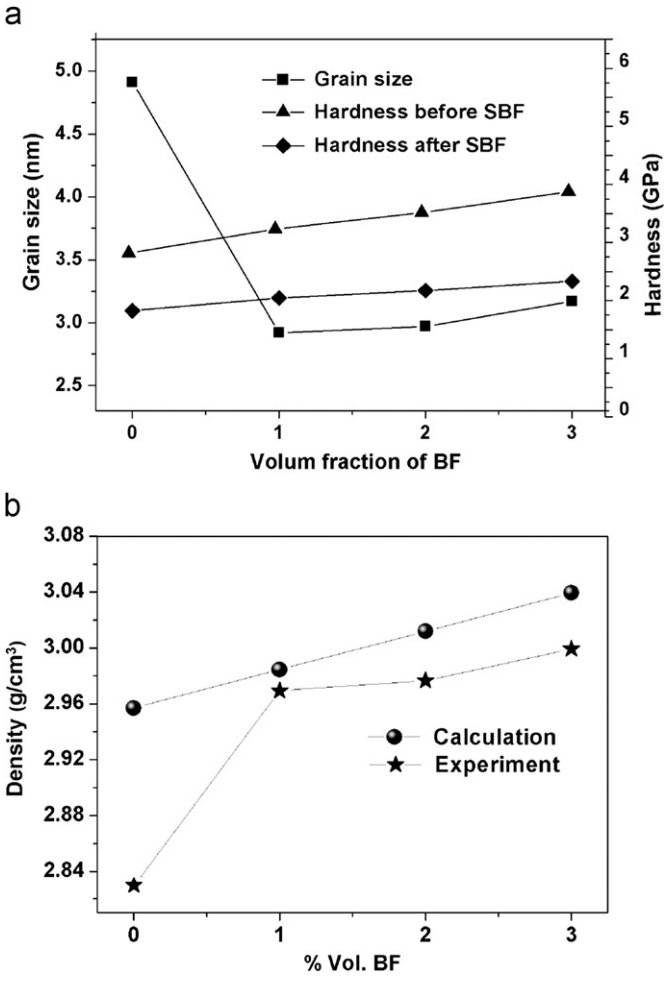

Fig. 3. (a) Grain size and hardness values versus BF content of the composites, (b) density versus BF content of the composites.

where the BF additive produced a decrease in the porosity. It should be noted that the porosity levels in SEM micrographs of the ceramic surfaces were consistent with the trend of measured density values. The density value, determined from the Archimedes method, increased with increasing BF content (Fig. 3(b)). Calculation density (ρ) of the composites can be estimated via the equation:

$$\rho = \sum_i \rho_i \frac{V_i}{V} \quad (1)$$

where the subscript i is number of phase in the composites and V is volume fraction of constituent phase. The calculated and experimental densities versus BF content are presented in Fig. 3(b).

It can be seen that the experimental densities are lower than that of calculated densities. This may be due to the close pores in the samples.

The variation of the average Vickers hardness values of the samples are shown in Fig. 3(a). The hardness values increased linearly with increasing BF content. This can be related to the density of the composites, i.e., the high density samples result in high measured hardness value. The reduction of grain is also considered to be another reason for increasing the hardness value where the smaller grain size samples gave the higher hardness values.

The magnic hysteresis loops of the composites measured at room temperature are presented in Fig. 4. An improvement in magnetic properties is clearly seen, due to the effect of BF content. Fig. 5 shows the values of the coercive magnetic field (H_c) and remnant magnetization (M_r) of the samples. The M_r value increased from 0.49 emu/g for the 1 vol% sample to 2.26 emu/g for the 3 vol% sample. The H_c also increased from ~365.4 Oe for the 1 vol% sample to 388.6 Oe for the 3 vol% sample.

For the bioactivity test, the obtained composites were immersed in the SBF for 14 days. Fig. 6 illustrates surfaces of the composites after soaking in the SBF. Round crystals of apatite precipitated (identified by energy-dispersive spectroscopy analysis) can be seen clearly. Areas of the round crystals increased with increasing BF content up to

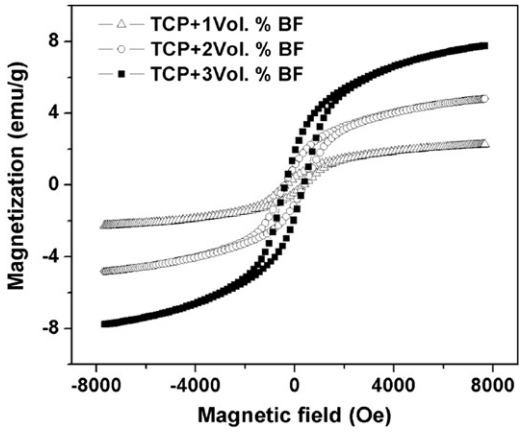

Fig. 4. Magnetization versus applied magnetic field of the composites.

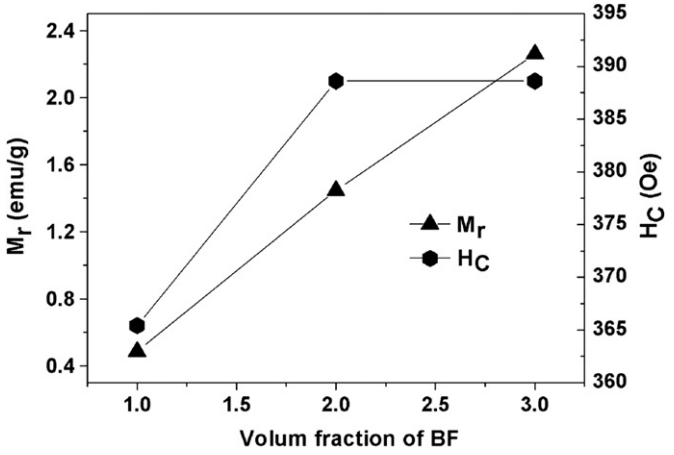

Fig. 5. Plots of M_r and H_c as a function of BF content.

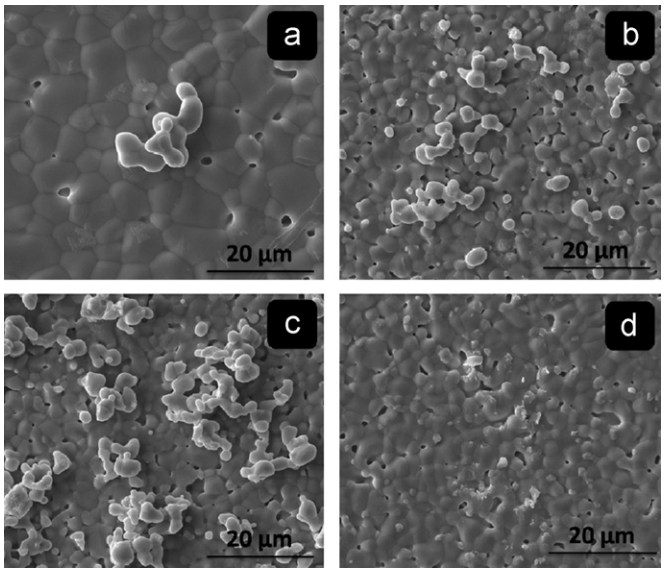

Fig. 6. Microstructure of the samples soaked in SBF solution: (a) β-TCP ceramic, (b) β-TCP −1.0 vol% BF,(c) β-TCP −2.0 vol% BF, and (d) β-TCP −3.0 vol% BF.

2.0 vol% BF. This result indicates that the apatite forming ability of the composites increased with increasing BF content, especially for the 2.0 vol% sample. However, the crystal did not form for the 3.0 vol% sample. Therefore, the surfaces of the studied composites are effective for inducing apatite formation in the body environment at some suitable BF contents. Hardness value of the composites measured after the bioactivity test was determined. The hardness values after bioactivity test were lower than that (shown in Fig. 3(a)) obtained before the test. Further, hardness value after the immersing slightly increased with BF content. This indicates a degradation of the sample surfaces after the bioactivity test. Based on the formation of apatite (Fig. 6), the 2.0 vol% sample may be suitable for biological applications.

4. Conclusion

In the present work, properties of β-TCP/BF composites were investigated for the first time. Additions of BF particles in the range 1–3 vol% to β-TCP were observed to suppress grain growth, resulting in an approximately 25% decrease in average grain size. The additive enhanced Vickers hardness values where it increased by up to ~13%, due to the additive decrease of porosity and grain size. The additive also produced the improvement in magnetic properties. The bioactivity test indicated that the 2.0 vol% sample had higher apatite forming ability. This material may be good for medical applications. However, further biological tests should be performed in future, to understand other biomaterial properties.

Acknowledgements

This work was supported by the Office of the Higher Education Commission (OHEC), Office of National Research Council of Thailand, Hands-on Research and Development Project; Rajamangala University of Technology Lanna, National Research Council of Thailand and the Faculty of Science and the Graduate School of Chiang Mai University.

References

[1] B. Viswanath, R. Raghavan, N.P. Gurao, U. Ramamurty, N. Ravishankar, Mechanical properties of tricalcium phosphate single crystal grown by molten salt systhesis, Acta Biomaterialia 4 (2008) 1448–1454.
[2] H.S. Ryu, H.J. Youn, K.S. Hong, B.S. Chang, C.K. Lee, S.S. Chang, An improvement in sintering property of β-tricalcium phosphate by addition of calcium pyrophosphate, Biomaterials 21 (2002) 909–914.
[3] S. Joschek, B. Nies, R. Krotz, A. Gopferich, Chemical and physicochemical characterization of porous hydroxyapatite ceramic made of natural bone, Biomaterials 21 (2000) 1645–1658.
[4] J. Chen, Y. Wang, X. Chen, L. Ren, C. Lai, W. He, Q. Zhang, A simple sol–gel technique for synthesis of nanostructured hydroxyapatite, tricalcuim phosphate and biphasic powder, Materials Letters 65 (2011) 1923–1926.
[5] Y. Li, W. Weng, K.C. Tam, Novel highly biodegradable biphasic tricalcium phosphate composed of α-tricalcium phosphate and β-tricalcium phosphate, Acta Biomaterialia 3 (2007) 251–254.
[6] A. Tampieri, T. Alessandro, M. Sandri, S. Sprio, E. Landi, L. Bertinetti, S. Panseri, G. Pepponi, J. Goettlicher, M.B. Lopez, J. Rivas, Intrinsic magnetism and hyperthermia in bioactive Fe-doped hydroxypatite, Acta Biomaterialia 8 (2012) 843–851.
[7] L. Wang, K.G. Neoh, E.T. Kang, B. Shuter, S.C. Wang, Biodegradable magnetic-fluorescent magnetite/poly (DL-lactic acid-co-α, β-malic acid) composite nanapaticles for stem cell labeling, Biomaterials 31 (2010) 3502–3511.
[8] Y. Liu, H. Zhong, L. Li, C. Zhang, Temperature dependence of magnetic property and photocatalytic activity of Fe_3O_4/hydroxyapatite nanopaticles, Materials Research Bulletin 45 (2012) 2036–2039.
[9] O. Kuda, N. Pinchuk, L. Ivanchenko, O. Parkhomey, O. Sych, M. Leonowicz, R. Wroblewski, E. Sowka, Effect of Fe_3O_4, Fe and Cu doping on magnetic properties and behavious in physiological solution of biological hydroxyapatite/glass composites, Journal of Magnetism and Magnetic Materials 209 (2009) 1960–1964.

[10] S.D. Castanon, J.L. Sanchez, E.E. Rams, F. Leccabue, B.F. Watts, Magneto-structural properties of $PbFe_{12}O_{19}$ hexaferrite powder prepared by decomposition of hydroxide carbonate and metal organic precipitate, Journal of Magnetism and Magnetic Materials. 185, 194–198.

[11] K. Du, H. Yang, R. Wei, M. Li, Q. Yu, W. Fu, N. Yang, H. Zhu, Y. Zeng, Electric-pulse discharge as a novel technique to synthesize-SiC nano-crystallites from liquid-phase organic precursors, Materials Research Bulletin 43 (2008) 120–126.

[12] S.J. Kalita, H.A. Bhatt, Nanocrystalline hydroxyapatite doped with magnesium and zinc synthesis and characterization, Materials Science and Engineering C 27 (2007) 837–848.

[13] P. Jarupoom, K. Pengpat, N. Pisitpipathsin, S. Eitssayeam, U. Intatha, G. Rujijanagul, T. Tunkasiri, Development of electrical properties in lead-free bismuth sodium lanthanum titanate–barium titanate ceramic near themorphotropic phase boundary, Current Applied Physics 8 (2008) 253–257.